

Spectroscopic Properties of Non-glycosylated Functional Unit KLH₂-c of Keyhole Limpet Hemocyanin

¹Aleksander Dolashki, ¹Jürgen Schütz, ²Rumyana Hristova, ¹Wolfgang Voelter and ²Pavlina Dolashka

¹Interfakultäres Institut für Biochemie, Hoppe-Seyler-Straße 4, D-72076 Tuebingen, Germany

²Institute of Organic Chemistry, Bulgarian Academy of Sciences, G. Bonchev 9, Sofia 1113, Bulgaria

Abstract: The functional unit KLH₂-c, isolated from the structural subunit KLH₂ of keyhole limpet *Megathura crenulata* hemocyanin, was studied to explain the effect of the oligosaccharide component for the conformational stability of the protein. The properties of this FU were characterized by fluorescence spectroscopy, combined with fluorescence quenching studies, using acrylamide, caesium chloride and potassium iodide as tryptophan quenchers. Using circular dichroism and fluorescence spectroscopy, the thermostability of the non-glycosylated FU KLH₂-c was studied in comparison to the glycosylated native molecule, the structural subunits KLH₁, KLH₂ and the FU RvH₁-a of *Rapana venosa* Hc. The melting T_m (45°C) as well as the critical temperatures T_c (46) were found to be less for KLH₂-c compared to the glycosylated forms which could be explained to be caused by the presence of oligosaccharide side chains and aggregation effects.

Key words: Circular dichroism • fluorescence spectroscopy • mollusc hemocyanins

INTRODUCTION

Hemocyanins (Hcs) are oxygen carriers and storage proteins of several species of molluscs and arthropods [1 - 3]. Their active site, positioned within hydrophobic pockets and shielded from external media, is of a binuclear-coupled type with copper ions, directly bound to six histidine nitrogens of the protein chain to which oxygen is bound reversibly [4].

The X-ray crystallographic studies of the functional unit (FU) from the molluscan hemocyanin of *Octopus dofleini* [5] have elicited a detailed picture from the protein's active site.

Keyhole limpet hemocyanin (KLH) is widely used in research and clinical studies. One present field of application is, for example, immunotherapy of bladder cancer [6 - 9], based on the assumed expression of Gal(β1-3)GalNAc determinants as cross-reacting epitopes [10]. Its potential application in anticancer therapy is under present investigation [11-13].

It is generally accepted that the oligosaccharide constituents of KLH are of prime significance for its antigenicity and biomedical properties and the carbohydrate structure of this glycoprotein. KLH is very heterogeneously glycosylated carrying preponderantly

high mannose-type glycans with 5-7 mannosyl hybrid-type species with five mannose residues and one *N*-acetylglucosamine chain. As a unique feature, the latter glycans carry, in part, a Gal(β1-6)Man determinant which has not been found in glycoprotein-N-glycans so far [14]. The present study further demonstrated the presence of a novel type of N-glycan exhibiting a Gal(β1-4)Fuc(α1-6)- or Gal(β1-4)Gal(β1-4)Fuc(α1-6)- core modification [15].

For this reason, the hemocyanin of the Californian giant keyhole limpet *Megathura crenulata* is well studied concerning the subunit structure, the number and arrangement of FUs, as well as the dissociation and reassembly behavior of both KLH isoforms [16 - 18]. KLH₁ apparently exists as a stable dodecamer with random clusters of didecamers [18, 19]. The quaternary structure of the KLH₁ didecamer has been provided from electron micrographs as well as the organization of FU of both KLH subunits, but little is known regarding its physical properties [20].

In the present study, we want to present some physical properties and the thermal stability of one non-glycosylated FU from keyhole limpet hemocyanin, KLH₂-c, in comparison with glycosylated structural subunits, the native KLH and hemocyanins from other molluscan species.

MATERIALS AND METHODS

Isolation of FU KLH2-c from keyhole limpet hemocyanin: KLH was obtained from Biosyn (Fellbach, Germany) with a protein concentration of 6.9 mg mL^{-1} in Tris/HCl buffer, pH 7.4. The sample was dialysed for 24 h against 0.1 M Tris/HCl buffer, pH 6.5, containing 1 mM CaCl_2 and 0.5 mM MgCl_2 .

The structural subunit KLH2 and FU KLH2-c were purified as described [20, 21]. Purity control and identification of the isolated functional unit KLH2-c were performed using SDS-PAGE (7.5% gel) and N-terminal sequence analysis.

Apo-Hc was prepared after 48 h dialysis of the native protein against 50 mM Tris-HCl buffer containing 20 mM EDTA and 20 mM KCN, pH 8.0, at 4°C . The fraction of oxy-Hc was determined spectrophotometrically by measuring the absorbance ratio at 340 and 278 nm and assuming the values $A_{340}/A_{278} = 0.21$ for the native, fully oxygenated proteins [2].

Spectroscopic methods: UV measurements: Absorption spectra were recorded with an Uvicon recording spectrophotometer. The concentrations were determined spectrophotometrically at 278 nm using as coefficient $E = 1.42 \text{ mL mg}^{-1} \text{ cm}^{-1}$. Molar concentrations were referred to 50 kDa as molecular mass for the species containing one binuclear copper site [2].

Fluorescence measurements: Fluorescence measurements were performed with a Perkin Elmer model LS 5 spectrofluorimeter, equipped with a thermostatically controlled assembly and a data station model 3600. The excitation wavelength was 295 nm and emitted light intensity was integrated over the period of 1 s and detected at 295-450 nm.

Fluorescence quantum yields were determined by the following equation [22]:

$$Q_x = Q_{st} (F_x / A_x) (A_{st} / F_{st}) (\lambda_x / \lambda_{st}) \quad (1)$$

where, Q_x , F_x and A_x are the emission quantum yield, the emission intensity at wavelength λ and the absorbance at the excitation wavelength, respectively, for the protein sample; Q_{st} , F_{st} and A_{st} are the same parameters for the reference standard. N-acetyltryptophanamide (Ac-Trp-NH_2) with a quantum yield of 0.13 was chosen as a standard [23]. The efficiency e of the tyrosine-to-tryptophan energy transfer was calculated using the relationship [24]:

$$Q = Q_{\text{Trp}} [f_{\text{Trp}}(\lambda) + e f_{\text{Tyr}}(\lambda)] \quad (2)$$

where, Q is the fluorescence quantum yield of the protein sample at the excitation wavelength, Q_{Trp} is the fluorescence quantum yield of the tryptophyl residues in the protein molecule after excitation at 300 nm and $f_{\text{Trp}}(\lambda)$ and $f_{\text{Tyr}}(\lambda)$ are the fractional absorption of tryptophan and tyrosine, respectively, at the excitation wavelength λ calculated from their molar ratio in the protein.

The results of the quenching reactions between the excited tryptophyl side chains and acrylamide were analyzed according to the Stern-Volmer equation [23]:

$$F_0 / F = 1 + K_{sv} [X] \quad (3)$$

where, F_0 and F are the fluorescence intensities at an appropriate emission wavelength in the absence and presence of quencher, K_{sv} is the quenching constant and $[X]$ the quencher concentration. The inner filter effect due to acrylamide was corrected by the factor:

$$Y = \text{antilog} (\text{Abs}_{\text{exc}} + \text{Abs}_{\text{emiss}}) / 2 \quad (4)$$

where, Abs_{exc} and $\text{Abs}_{\text{emiss}}$ are the absorbances at the excitation and emission wavelength, respectively.

CD measurements: Circular dichroism was measured with a Jasco J-720 dichrograph, equipped with a personal computer IBM PC-AT, PS/2, multiscan monitor CMS-3436 and a Hewlett-Packard color graphics plotter model HP 7475A. A software DOS version was used for calculation of the CD data. Protein solutions in 50 mM Tris/HCl buffer, 10 mM CaCl_2 , pH 8.0 were thermostatically controlled using a NESLAB thermostat model RTE-110, connected with a digital programming controller. The temperature inside the cuvette was monitored with a thermocouple.

Temperature stability: The temperature dependence of the Hc fluorescence was determined at pH 8.0 in 0.05 M Tris/HCl, 10 mM CaCl_2 buffer. 0.2 mg of the samples were kept for 10 min at the desired temperature prior to the measurement, to ensure the attainment of thermal equilibration. The critical temperature (T_c) and melting temperature (T_m) values were calculated from the circular dichroism or fluorescence spectroscopy data.

RESULTS AND DISCUSSION

Isolation of FU KLH2-c: The structural subunits KLH1 and KLH2 were isolated as described previously [20].

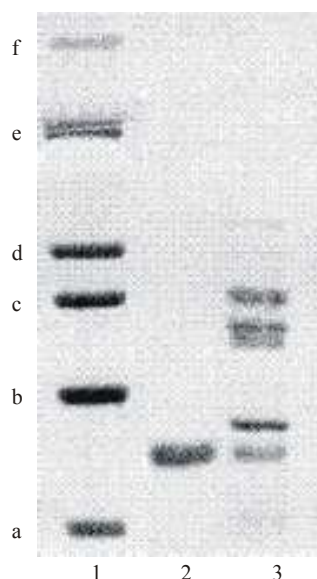


Fig. 1: Native PAGElectrophoresis (10% gel) of native hemocyanin and its subunits: Lane 1 - standard sample; lane 2 - FU KLH2-c; lane 3 - tryptic digestion of KLH2

The electrophoretically pure functional unit KLH2-c was isolated from the structural subunit KLH2 as described by Shuetz *et al.* [20]. The purity of KLH2-c was checked on 10% gel which shows only one fraction with a molecular mass of about 45 kDa (Fig. 1, lane 2).

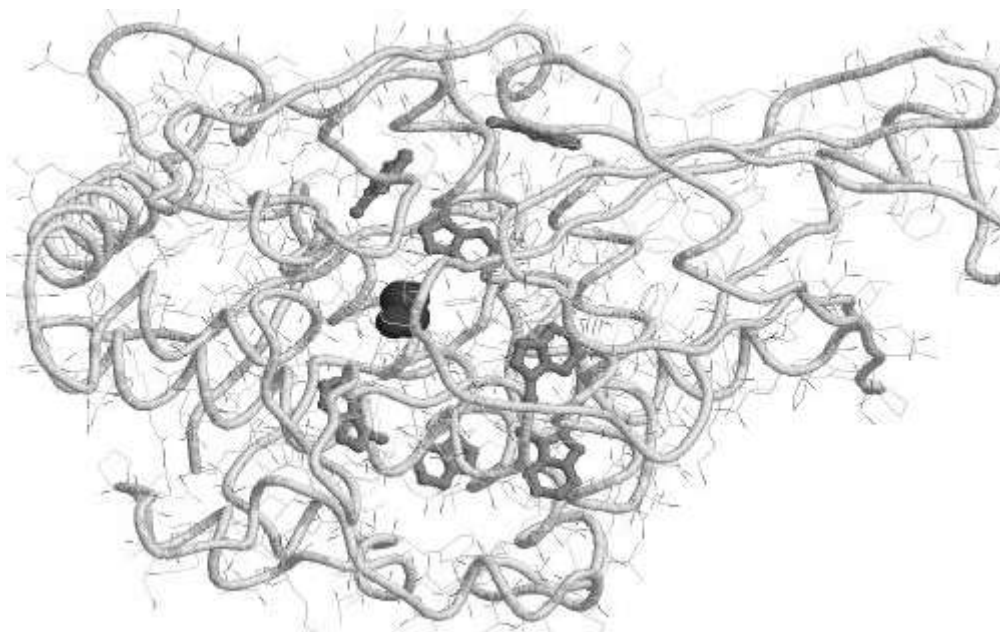
Fluorescence properties: The properties of FU KLH2-c were characterized using the very sensitive method of fluorescence spectroscopy and the results were compared with those from the structural subunits KLH1 and KLH2 as well as with the functional unit RvH1-a, isolated from *Rapana venosa* hemocyanin (renamed from *Rapana thomasi*) [5]. Fluorescence parameters of KLH2-c show that after excitation at 280 nm, where phenol and

indole groups absorb, or at 295 nm, where at last 93% of the incident light is absorbed by the tryptophyl residues, oxy-KLH2-c exhibits an emission spectrum with a maximum (λ_{\max}) at 335.5 ± 1 (Table 1) which is typical for “buried” tryptophyl side chains in a non-polar environment. These results are in agreement with those found for the native molecule, its subunits KLH1, KLH2 and FU RvH1-a with λ_{\max} values of 330.5 ± 1 , 336 ± 1 , 335 ± 1 and 331 nm, respectively [20]. The wavelength of emission maximum increases by 1-2 nm comparing the oxy- with the apo-Hc, suggesting that the removal of copper and peroxide slightly change the environment of the tryptophan residues. In addition, the quantum yield increased slightly (from $Q_{\text{oxy-}} = 0.046$ to $Q_{\text{apo-}} = 0.075$) which could be explained by the longer distances between Cu ions and the Trp residues influence including slightly on the copper-peroxide complex. Figure 2 shows the positions of Trp residues which are located within long distance from the active site of *Octopus deflieni* FU Odg. These results fit very well to the published results for the whole molecule, structural subunits KLH1 and KLH2 and FU RvH1-a ($Q_{\text{oxy-}} = 0.036$; $Q_{\text{apo-}} = 0.068$; $Q_{\text{oxy-}} = 0.042$; $Q_{\text{apo-}} = 0.070$; $Q_{\text{oxy-}} = 0.060$; $Q_{\text{apo-}} = 0.074$; $Q_{\text{oxy-}} = 0.051$; $Q_{\text{apo-}} = 0.072$, respectively) (Table 1). This effect is more evident in the case of oxy-forms, probably because the copper-peroxide complex of oxy-Hc quenches selectively buried tryptophan residues. It can be concluded that the fluorescence emission of both, oxy- and apo-forms of native KLH, its structural subunits and FU KLH2-c are dominated by deeply buried tryptophyl side chains.

This conclusion is further supported by quenching experiments with neutral and ionic quenchers. Fluorescent quenching reactions have been widely used for studying the degree of exposure and environment of aromatic amino acid residues. The fluorescent quenching experiments were performed in 50 mM Tris/HCl buffer, 10 mM CaCl_2 , pH 8.0 with different concentrations of

Table 1: Fluorescence parameters of FUs KLH2-c and RvH1-a, whole molecule KLH and its structural subunits

Species	Emission λ_{\max} [nm]	Quantum yield (Q)	Tyr to trp energy transfer e (%)	Acrylamide quenching $K_{\text{SV}}(\text{M}^{-1})$	KI quenching $K_{\text{SV}}(\text{M}^{-1})$	CsCl quenching $K_{\text{SV}}(\text{M}^{-1})$	E ($K_{\text{SV-}}/K_{\text{SV+}}$)
Native oxy-	330 \pm 1	0.036	65	2.28	1.30	0.880	1.47
KLH apo-	332 \pm 1	0.068					
KLH1 oxy-	336 \pm 1	0.042	25	3.39	1.25	0.709	1.76
KLH1 apo-	338 \pm 1	0.070					
KLH2 oxy-	335 \pm 1	0.060	40	3.01	1.10	0.500	2.20
KLH2 apo-	336 \pm 1	0.074					
KLH2-c oxy-	335 \pm 1	0.046	43	3.59	1.35	0.920	1.70
KLH2-c apo-	337 \pm 1	0.075					
RvH1-a oxy-	331 \pm 1	0.051	23	5.01	2.40	1.200	2.00
RvH1-a apo-	333 \pm 1	0.072					
Ac-Trp-NH2	350 \pm 1	0.130	1.25	16.33	8.80	2.000	4.40



Distances between CuA/CuB and Trp residues in FU Odg from *Octopus dofleini* hemocyanin (to atoms CZ) in Å°

Trps	74	98	100	191	222	226	360
CuA	7.92	11.02	10.60	13.84	12.32	17.24	13.14
CuB	5.33	14.21	12.07	16.68	12.78	18.62	10.24

Fig. 2: X-ray model of FU Odg. Distances between CuA/CuB and Trp residues in FU Odg from *Octopus dofleini* hemocyanin (to atoms CZ) in Å°

acrylamide. Acrylamide is an efficient neutral quencher of tryptophan fluorescence and the discrimination between "buried" and "exposed" residues can be based on the values of the Stern-Volmer quenching constant (K_{sv}) of Eq. (3). The Stern-Volmer quenching plots (Fig. 3), described by Eq. (3), for the different samples are linear, allowing to determine single K_{sv} constants (values are given in Table 1).

Two classes of "buried" fluorophores can be considered to be responsible for the Hc fluorescence: first, Trp residues localized very close to the active site pocket and second, Trp moieties involved in inter-subunits contacts. From the X-ray structure of Odg FU it becomes obvious that the Trp residues are "buried" in the molecule which is confirmed by results Fig. 2. The quenching efficiencies K_{sv} 2.28, 3.01 and 3.39 M^{-1} , calculated for oxy- native KLH and its structural subunits KLH1 and KLH2 respectively, are very low compared to $K_{sv} = 16.33 M^{-1}$ of tryptophan in aqueous solution and indicate that the tryptophyl side chains are deeply

buried in hydrophobic regions of the hemocyanin aggregates. The K_{sv} values of the FUs KLH2-c and RvH1-a (Table 1, $K_{sv} = 3.59$ and $5.01 M^{-1}$, respectively), are larger compared to the K_{sv} of the native hemocyanin ($2.28 M^{-1}$) and we suggest that the tryptophyl side chains in oligomeric subunits as well as in the native molecule are similarly "buried".

The X-ray crystal structure of the functional unit of Octopus Hc Odg shows that it contains seven tryptophan residues, located around the active site, while only six Trp residues were identified for the amino acid sequence of KLH2-c located at positions 51, 74, 98, 100, 223 and 226. Alignment of the amino acid sequences of the Hc-FUs of Octopus dofleini Odg and KLH2-c shows that the positions of five Trp residues are conserved, but they are not part of the copper active sites (Fig. 1A). Only one of the Trp residues is located close to the CuB site.

The conclusion that Trp residues are exposed inside the molecule is supported also by the results of the quenching experiments with the ionic species Cs^{+} and I^{-} .

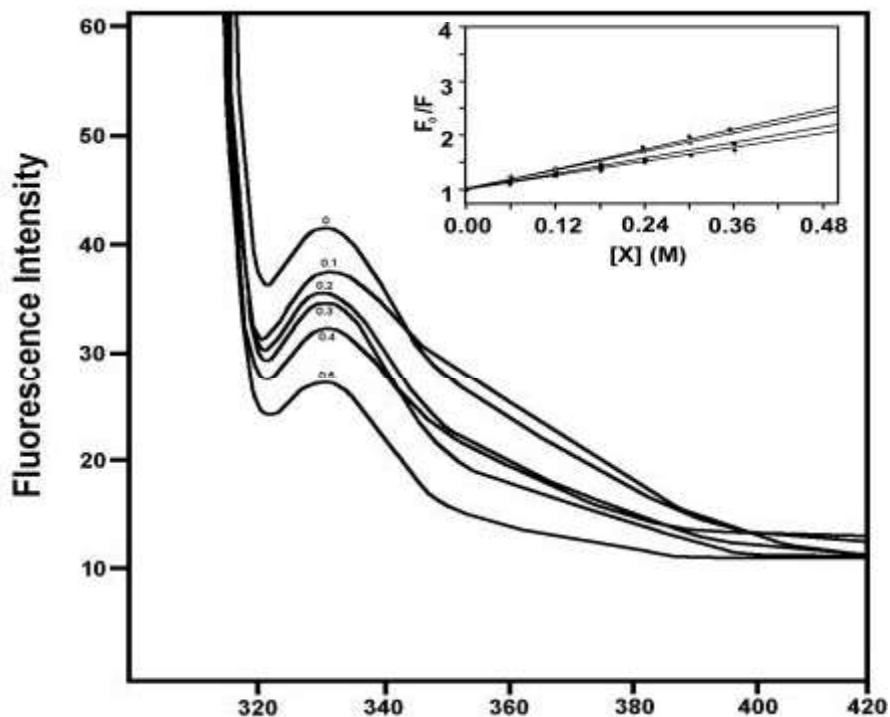


Fig. 3: Stern-Volmer plots for fluorescence quenching with acrylamide of KLH and its structural subunits performed at 25°C after excitation of the samples at 295 nm: KLH2-c (◆—◆), KLH (■—■), KLH1 (●—●), KLH2 (○—○).

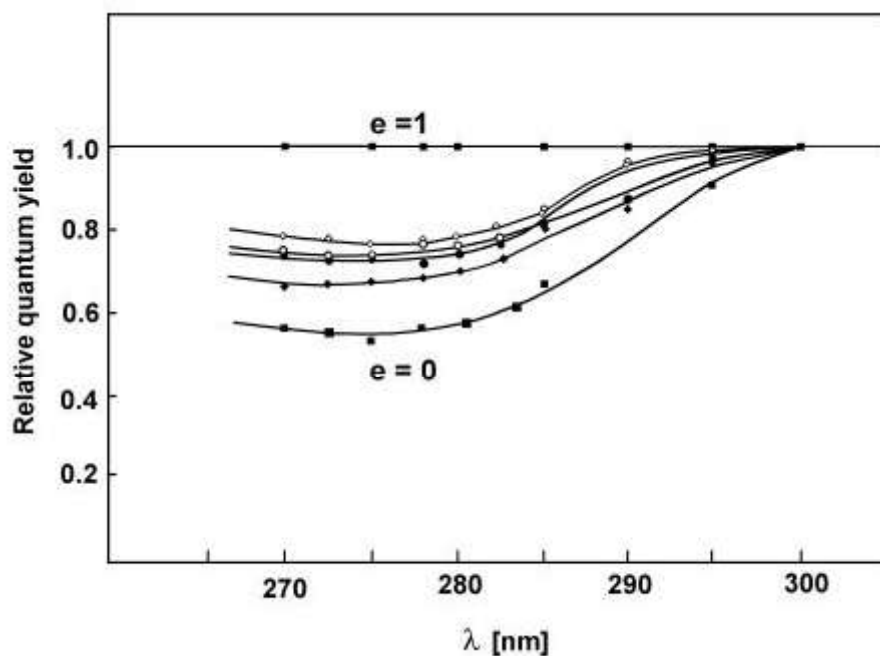


Fig. 4: Tyrosine to tryptophan energy transfer efficiency of the apo-structural subunit: KLH1 (◆—◆), KLH2 (●—●), KLH2-c (○—○) and native Hc (?—?). The upper (■—■) and lower (■—■) solid curves are the theoretical and obtained from different values of the transfer efficiency ($e = 1$ and 0 , respectively)

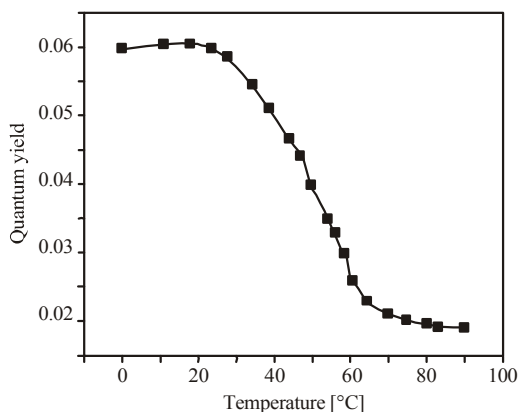


Fig. 5: Thermal dependence of the tryptophyl fluorescence of the FU KLH2-c in 50 mM Tris/HCl, 10 mM CaCl₂ buffer, pH 8.0. The fluorescence quantum yield was determined using N-Ac-Trp NH₂ as a standard

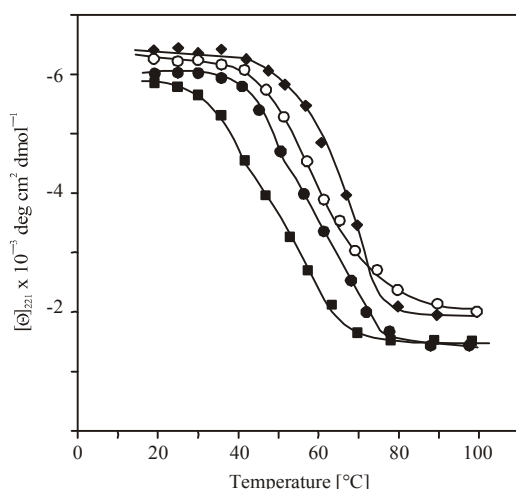


Fig. 6: Temperature dependences of the ellipticity $[\Theta]$ at 221 nm of native KLH (◆—◆), its structural subunits: KLH1 (●—●), KLH2 (○—○) and FU KLH2-c (■—■), were determined in 0.05 M Tris/HCl, 10 mM CaCl₂, 10 mM MgCl₂ buffer, pH 8.0

In contrast to acrylamide, which can penetrate the protein matrix, the ionic quenchers are hydrated and cannot diffuse into the protein molecule. They only are able to quench surface fluorophores, although complication may arise from the electric potential around the fluorophore, since the quenchers have a positive or a negative charge. The quenching constant of the ionic species is very low for KLH2-c (Table 1; $K_{sv} = 0.92 \text{ M}^{-1}$ for Cs⁺ and 1.35 M^{-1} for I⁻) compared to the constants for free tryptophan

(Table 1) 2.0 M^{-1} (for Cs⁺) and 8.8 M^{-1} (for I⁻). These data are again consistent with the results obtained for the other samples and support the conclusion that the tryptophyl side chains are "buried" in the native hemocyanin aggregate and its functional subunits. The ratio of the Stern-Volmer constants, determined for the negative and positive quencher (K_{sv-}/K_{sv+}), defines an electrostatic parameter E , sensitive to the charge in the microenvironment around the fluorophore. The value for the dodecameric Hc ($E = 1.47$, Table 1) is lower compared to that found for the structural subunits ($E = 1.76$ and $E = 2.2$) and FUs (KLH2-c and RvH1-a 1.7 and 2.0, respectively).

The absence of a tyrosyl fluorescence, which can be expected at 303 nm, can be explained on the basis of an energy-transfer process involving phenol (energy donors) and indole (energy acceptors) groups [26]. The X-ray models of *Octopus dofleini* [5] demonstrate many possibilities for an efficient Tyr to Trp energy transfer. In Fig. 4 the typical plots, used to calculate the Tyr-Trp energy transfer efficiency according to Eq. (2) is shown for the FU KLH2-c, subunits KLH1, KLH2 and the native molecule. The corresponding e values are summarized in Table 1. The best fit of the experimental data to the theoretical curves was obtained for $e = 0.43$ for the FU, 0.65 for the dodecameric Hc and between 0.40-0.25 for the structural subunits. It can be concluded that about 40% of the light absorbed by the tyrosyl residues in the FU KLH2-c and 25-40% in the subunits is transferred to indole rings and emitted as tryptophan fluorescence.

Conformational stability of the FU KLH2-c: Temperature denaturation: Thermostability is an important property of biomolecules, especially regarding their practical application. The stability of Fu KLH2-c was studied using fluorescence spectroscopy in comparison to native KLH, its subunits KLH1 and KLH2 and the FU RvH1-a in the range from 20 to 95°C in 50 mM Tris/HCl, 10 mM CaCl₂, pH 8.0 (Fig. 5). The data were collected for the apo-forms only, because oxygen saturation of Hcs is temperature-dependent. The critical transition temperature T_c is determined from the Arrhenius plot as the temperature at which a change in the slope of the plot occurs. As expected, the T_c parameters 46 and 49°C, determined for the FUs KLH2-c and RvH1-a, respectively are smaller compared to the dodecameric Hc (63°C) and its subunits (51-53°C) (Table 2). As the thermal denaturation of the Hc species after passing the T_c was irreversible, equilibrium thermodynamic parameters were not determined.

Table 2: Thermostability of FUs KLH2-c and RvH1-a, natural KLH and its structural subunits

Species	Fluorescence T _c (°C)	CD T _m value
Native KLH	63	67
KLH1	53	56
KLH2	51	52
KLH ₂ -c	46	45
RtH1-a	49	49

The thermal denaturation study was complemented by CD measurements of the apo-forms of the individual subunits. In the far UV region, a minimum was observed at 208 and 221 nm, which is characteristic for the secondary structures of the proteins. The spectra were recorded at a temperature interval 20 - 90°C in the 200 - 260 nm region, reflecting the backbone conformation of proteins. A sigmoidal curve was obtained for apo-forms when the ellipticity at 221 nm was plotted as a function of temperature (Fig. 6). The melting temperature (T_m 45 and 49°C) for the FUs KLH2-c and RvH1-a, respectively, are smaller compared to native KLH and its structural subunits (67, 56 and 52°C, respectively) and are in agreement with the T_c values, obtained by fluorescence spectroscopy. Table 2 summarizes the melting temperatures of native isoforms of *Megathura crenulata* hemocyanin and FU RvH1-a [25], which confirm that the two molluscan Hcs are similar in thermostability.

The high conformational stability of molluscan Hcs could be due to the larger number of disulphide bridges. However, the possibility of a structural role of the sugar moieties in molluscan hemocyanins cannot be excluded. Two carbohydrate binding N-linked site were identified in the FU RvH1-a and a carbohydrate content of 4,19% were determined [28], while no oligosaccharides was found to be present in FU KLH2-c.

ACNOWLEDGEMENTS

The present work was granted by National Found for Scientific Research (grant X-1202) and Dr. P. Dolashka-Angelova thanks to DFG for granting a scholarship.

REFERENCES

1. Van Holde, K.E. and K.I. Miller, 1995. Hemocyanins. *Adv. Protein. Chem.*, 47: 1-81.
2. Salvato, B. and M. Beltramini, 1990. Hemocyanins: Molecular architecture, structure and activity of the binuclear copper active site. *Life Chem. Rep.*, 8: 1-47.
3. Harris, J.R. and J. Markl, 1999. Keyhole limpet hemocyanin (KLH): A biomedical review. *Micron*, 30: 597-623.
4. Solomon, E.I., M.J. Baldwin and M.D. Lowery, 1992. Electronic structures of active sites in copper proteins: Contributions to reactivity. *Chem. Rev.*, 92: 521-542.
5. Cuff, M.E., K.I. Miller, K.E. van Holde and W.A. Hendrickson, 1998. Crystal structure of a functional unit from *Octopus* hemocyanin. *J. Mol. Biol.*, 278: 855-870.
6. Harris, J.R. and J. Markl, 2000. Keyhole limpet hemocyanin: Molecular structure of a potent Marine immunoactivator. *Eur. Urol.*, 37: 24-33.
7. Jurincic-Winkler, C.D., K.A. Metz, J. Beuth and K.F. Klippel, 2000. Keyhole Limpet Hemocyanin for Carcinoma in situ of the Bladder: A Long-Term Follow-Up Study. *Eur. Urol.*, 37: 45-49.
8. Lamm, D.L., J.I. Dehaven and D.R. Riggs, 2000. Keyhole Limpet Hemocyanin Immunotherapy of Bladder Cancer: Laboratory and Clinical Studies. *Eur. Urol.*, 37, 3: 41-44.
9. Mansour, M.A., P.O. Ali, Z. Farid, A.J.G. Simpson and J.W. Woody, 1989. Serological differentiation of acute and chronic schistosomiasis mansoni by antibody responses to keyhole limpet hemocyanin. *Am. J. Trop. Med. Hyg.*, 41: 338-344.
10. Alves-Brito, C.F., A.J.G. Simpson, L.M.G. Bahia-Oliveira, A.L.T. Rabello, R.S. Rocha, J.R. Lambertucci, G. Gazzinelli, N. Katz and R. Correa-Oliveira, 1992. Analysis of anti-keyhole limpet hemocyanin antibody in Brazilians supports its use for the diagnosis of acute schistosomiasis mansoni. *Trans. R. Soc. Trop. Med. Hyg.*, 86: 53-56.
11. Wirguin, I., L. Suturkova-Milosevic, C. Briani and N. Latov, 1995. Keyhole limpet hemocyanin contains Gal (β 1-3)GalNAc determinants that are cross-reactive with the T-antigen. *Cancer Immunol. Immunotherapy*, 40: 307-310.
12. Gilewski, T., S. Adluri, G. Ragupathi, S. Zhang, T.J. Yao, K. Panageas, M. Moynahan, A. Houghton, L. Norton and P.O. Livingston, 2000. Vaccination of high-risk breast cancer patients with mucin-1 (MUC1) keyhole limpet hemocyanin conjugate plus QS-21. *Clin. Cancer. Res.*, 6: 1693-1701.
13. Krug, L.M., G. Ragupathi, K.K. Ng, C. Hood, H.J. Jennings, Z. Guo, M.G. Kris, V. Miller, B. Pizzo, L. Tyson, V. Baez and P.O. Livingston, 2004. *Clin. Cancer. Res.*, 10: 916-923.
14. Kurokawa, T., M. Wuhler, G. Lochnit, H. Geyer, J. Markl and R. Geyer, 2002. Hemocyanin from the keyhole limpet *Megathura crenulata* (KLH) carries a novel type of N-glycans with Gal(beta1-6)Man-motifs. *Eur. J. Biochem.*, 269: 5459-5473.

15. Wuhrer, M., M.L. Robijn, C.A. Koeleman, C.I. Balog, R. Geyer, A.M. Deelder and C.H. Hokke, 2004. A novel Gal(beta1-4)Gal(beta1-4)Fuc(alpha1-6)-core modification attached to the proximal N-acetylglucosamine of keyhole limpet haemocyanin (KLH) N-glycans. *Biochem. J.*, 378: 625-632.
16. Swerdlow, R.D., R.F. Ebert, P. Lee, C. Bonaventura and K.I. Miller, 1996. Keyhole limpet hemocyanin: Structural and functional characterization of two different subunits and multimers, *Comp. Biochem. Physiol.*, 113B: 537-548.
17. Markl, J., A. Savel-Niemann, M. Wegener-Strake, A. Sueling, W. Schneider, J. Gebauer and R. Harris, 1991. The role of two distinct subunit types in the architecture of keyhole limpet hemocyanin (KLH), *Naturwiss.*, 78: 512-512.
18. Harris, J.R., W. Gebauer, S.M. Soehngen and J. Markl, 1995. Keyhole limpet haemocyanin (KLH): Purification of intact KLH1 through selective dissociation of KLH2, *Micron*, 26: 201-212.
19. Harris, J.R., W. Gebauer, S.M. Soehngen, M.V. Nermut and J. Markl, 1997., Keyhole limpet hemocyanin (KLH). II: Characteristic reassociation properties of purified KLH1 and KLH2, *Micron*, 28: 43-56.
20. Schütz, J., P. Dolashka-Angelova, R. Abrashev, P. Nicolov and W. Voelter, 2001. Isolation and spectroscopic characterization of the structural subunits of keyhole limpet hemocyanin. *Biochim. Biophys. Acta*, 1546: 325-336.
21. Kirby, E.P. and R.F. Steiner, 1970. The tryptophan microenvironment in apomyoglobin. *J. Biol. Chem.*, 245: 6300-6306.
22. Lehrer, S.S., 1971. Solution perturbation of protein fluorescence. The quenching of the tryptophyl fluorescence of model compounds and of lysozyme by iodide ion, *Biochemistry*, 10: 3254-3263.
23. Eisinger, J., 1969. Intramolecular energy transfer in adrenocorticotropin, *Biochemistry*, 8: 3902-3907.
24. Stoeva, S., J. Schutz, W. Gebauer, T. Hundsdoerfer, C. Manz, J. Markl and W. Voelter, 1999. Primary structure and unusual carbohydrate moiety of functional unit 2-c of keyhole limpet hemocyanin (KLH). *Biochim. Biophys. Acta*, 1435: 94-109.
25. Dolashka-Angelova, P., M. Schick, S. Stoeva and W. Voelter, 2000. N-terminal functional unit of subunit R_tH₁ from *Rapana thomasiana* grosse hemocyanin. *Intl. J. Biochem. & Cell Biol.*, 32: 529-538.
26. Stryer, L., 1978. Fluorescence energy transfer as a spectroscopic ruler, *Ann. Rev. Biochem.*, 47: 819-846.
27. Ricchelli, F., G. Jori, L. Tallandini, P. Zatta, M. Beltramini and B. Salvato, 1984. The role of copper and quaternary structure on the conformational properties of *Octopus vulgaris* hemocyanin, *Arch. Biochem. Biophys.*, 235: 461-469.
28. Dolashka-Angelova, P., A. Beck, A. Dolashki, M. Beltramini, S. Stevanovic, B. Salvato and W. Voelter, 2003. Characterization of the carbohydrate moieties of the functional unit R_vH1-a of *Rapana venosa* haemocyanin using HPLC/electrospray ionization MS and glycosidase digestion. *Biochem. J.*, 374: 185-192.